



# Hydrogen Evolution on Zeolite Supported Platinum Clusters\*\*

S. Mentus<sup>1\*</sup>, Z. Mojovic<sup>1</sup>, N. Cvjeticanin<sup>1</sup> and Z. Tesic<sup>2</sup>

<sup>1</sup> Faculty of Physical Chemistry, Belgrade University, Studentski trg 12, 11000 Belgrade Yugoslavia

<sup>2</sup> Faculty of Chemistry, Belgrade University, Studentski trg 12, 11000 Belgrade Yugoslavia

Received 28.01.03, in revised form 26.03.03, accepted 07.04.03

## Abstract

NaX type zeolite was loaded with platinum, by the thermal decomposition of Pt(II) acetylacetonate, up to the Pt/NaX mass ratio of 0.174. The sample, dispersed on a glassy carbon rotating disc, was used in slightly acidic solution to observe the kinetics of the hydrogen evolution reaction. A comparison was made with the rate of hydrogen evolution on

smooth polycrystalline platinum, and both slower and faster evolution rates were observed, depending on the percentage of carbon black added to the zeolite sample.

**Keywords:** Catalysis, Hydrogen Evolution, Platinum Clusters, Rotating Electrode, Zeolite

## 1 Introduction

Zeolites are crystalline aluminosilicates having a porous, cavity structure with a very developed specific surface area, amounting to several hundred square meters. Their basic structural units are SiO<sub>4</sub> and AlO<sub>4</sub> tetrahedra, conjoined in a solid three-dimensional network [1]. In the zeolite crystal network, one can distinguish the caves and the channels, the dimensions of which depend on the type of zeolite. The negative charge of the aluminosilicate network is usually compensated for by alkali (in synthetic zeolites) or alkali-earth (in natural zeolites) cations. These cations can be replaced by cations of other metals by an ion-exchange procedure. Molecules having a diameter lower than the cavity entrance, may be adsorbed strongly and in high quantities inside the cavities, while those having a higher diameter may be adsorbed in a negligible amount on the outer crystal surface only. This is why zeolites are also named molecular sieves.

The metal salts, particularly those of transition or noble metals, introduced to the zeolite cavities, may be reduced to metal clusters of nanoscale dimensions. The catalytic effectiveness of such systems in numerous, particularly organic, chemical reactions is well known and has been the subject of recent investigations [2 – 8]. Their catalytic activity is discussed in terms of electron deficiency caused by the presence of alkali cations around the metal clusters [3]. There are numerous investigations, based on the electron microscopy technique, relating to the size, shape, and location of metal moieties in zeolite cavities [9 – 13] and in silicate based mesoporous materials [14]. Clusters containing 5 – 12 Pt atoms can

also be identified by extended X-ray adsorption fine structure spectroscopy (EXAFS) [15, 16]. A solid aluminosilicate framework hinders cluster agglomeration [17]. Recently Simon [18] reviewed the electrical properties of nanoscaled host/guest compounds involving zeolite guests.

From an electrochemical viewpoint, zeolites were investigated in the following ways: (i) pasted with graphite powder and fixed (by a small amount of polymeric binder) on a smooth metal or carbon surface, in order to investigate its influence on the kinetics of the electrochemical reaction of electroactive species from the surrounding solution, such as hydrazine, alcohol or hydroquinone oxidation [19], (ii) modified by incorporating the electroactive species inside the cavities, and fixed on the metal or carbon surface, in order to investigate the kinetics of the redox processes of the species inside the cavities, for example MV/MV<sup>2+</sup> (MV = methylviologen) [20] and Fe<sup>2+</sup>/Fe<sup>3+</sup> [21]. (iii) modified by incorporating Pt clusters and dispersed in a low conductive media, to act as bipolar electrodes in a static electric field [22].

Recently much effort has been invested in finding an effective catalyst, able to accelerate the electrode reactions in fuel cells. Platinum or its alloys dispersed on very fine carbon particles is widely used in this sense [23 – 26]. The high surface area carbon support (> 70 m<sup>2</sup> g<sup>-1</sup>) serves to suppress the

[\*] Corresponding author, slavko@ffh.bg.ac.yu

[\*\*] The paper has been presented at Symposium 8 of the International Society of Electrochemistry in Düsseldorf, Germany 2002

agglomeration of fine platinum particles during preparation and catalyst action. In this work, zeolite 13 X (faujasite type) was used to support platinum particles, in order to investigate the kinetics of hydrogen evolution on this material.

## 2 Experimental

### 2.1 Sample Preparation

After removal of almost all adsorbed water by heating at 350 °C and cooling within a closed vessel, a sample of zeolite NaX (Linde Co.) was wetted with a dilute acetone solution of platinum(II) acetylacetonate, dried at 90 °C to evaporate acetone, and heated at 350 °C, in order to decompose the platinum complex and desorb the decomposition products. The procedure was repeated until a Pt/zeolite weight ratio of 0.174 was reached. During this procedure the colour of the starting powder changed from white to dark-brown.

### 2.2 Methods of Sample Characterization

The morphology of the zeolite powder before and after modification by platinum incorporation was observed with a scanning electron microscope (JEOL 840A). The water content of the original and modified samples was controlled by a thermo-analytical device (TA Instruments Model SDT 2960).

Since one is dealing with powdery materials, the electrical conductivity of the samples was measured within a cylindrical die, made of insulating organic glass, reinforced outside by a stainless cylinder. The sample, usually 1 mm thick, was pressed between two stainless pistons, which were connected to the impedance measurement system. The impedance was measured under constant pressure, either 700 or 1400 kg cm<sup>-2</sup>, using either the PAR Model 384 device, which enabled measurements within the frequency range 1 mHz to 100 kHz, or the Wayne Kerr bridge Model 244, equipped with an external source of sinusoidal voltage, enabling reliable impedance measurements within the frequency range 0.4 – 40 kHz. The amplitude of the sinusoidal voltage was 10 mV in the case of the PAR device, and 500 mV when Wayne Kerr bridge was used. Usually, 5 points per decade of frequency was used to plot the impedance diagrams.

### 2.3 Electrochemical Measurements

By means of an ultrasonic bath, the powdery zeolite samples were dispersed in N-methyl-2-pyrrolidone (Johnson-Matthey GmbH) in which 2% poly(vinylidene) fluoride was dissolved. A droplet of this suspension was placed on a glassy carbon disc which was part of a rotating electrode with teflon insulation. The diameter of the disc was 3 mm. The solvent was removed by heating at 90 °C. After drying, the zeolite particles remained bonded to the glassy carbon surface. This way is otherwise the usual for preparing dispersed materials, for instance Li-intercalate powders [24, 25], to investigate electrochemical behaviour. In such a manner, an

approximate electrode coverage of 1 mg cm<sup>-2</sup> with zeolite supported platinum was obtained. Alternatively, 5 or 10 wt.% carbon black Vulcan XC72R (Cabot Corp.) was added to the initial suspension, in order to improve the electrical contact between the zeolite particles and the glassy carbon support.

The glassy carbon disc, on which a thin layer of Pt-modified zeolite was applied, was used as a working electrode in a thermostatted three-electrode electrochemical cell. The reference electrode was a saturated calomel electrode (SCE), and a wide platinum foil was used as the counter electrode. The electrolyte was an aqueous solution of Na<sub>2</sub>SO<sub>4</sub> (1 M) and 2.5 mM H<sub>2</sub>SO<sub>4</sub>. An argon stream deaerated the cell. The device used for electrochemical measurements was a PAR EG&G Potentiostat/Galvanostat Model 273. The polarization curves were recorded within the potential interval 0.0 V to -1.1 V vs SCE, at various polarization and rotation rates.

## 3 Results and Discussion

### 3.1 Sample Characterization

The size of the crystals of various commercial zeolites depends on the synthesis conditions, and samples of different degrees of crystallization, also involving the amorphous phase, may be produced. The SEM micrograph of the zeolite 13X used in this work (Figure 1) shows that it is crystalline, with a rather uniform particle diameter of approx. 3 μm. The x-ray diffractograms and structural details of this zeolite are well known and available in the atlases of crystallographic data for faujasite (FAU) type zeolites. Its larger cavity diameters of approx. 1.3 nm enable many large organic and complex molecules to enter inside the cavities. Regular SEM micrographs do not display any difference between the original and the platinum modified samples.

Formerly, metal clusters of either noble or transition metals, were incorporated in zeolite cavities by an ion exchange procedure, followed by the chemical reduction of the incor-

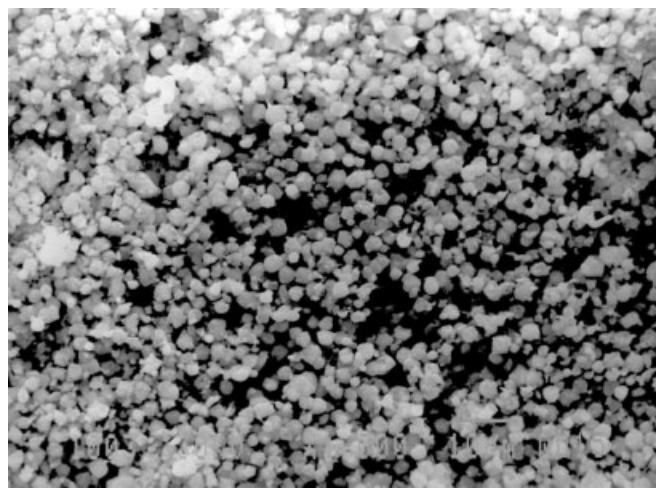


Fig. 1 SEM photograph of modified zeolite 13 X. The length of the photograph corresponds to 110 μm.

porated metal cations to metal atoms [22, 29]. Such a procedure may cause the zeolite crystal network to be destroyed, since it affects its regular cation/anion mole ratio. The procedure used in this work avoids this, since platinum is introduced into the zeolite framework as a neutral organic complex, which doesn't cause ion exchange. Therefore, the original zeolite structure remains intact.

The Pt/zeolite mass ratio of 0.174, of the sample under investigation, is slightly lower than the equilibrium water/zeolite mass ratio in free air, amounting to 0.2 – 0.33. Having the ratio of the relative molar masses of water (ice) and platinum (18:195) in mind, one may conclude that in this sample less than 1/10, approximately, of the inner cavity volume, which may be occupied by water, was now occupied by platinum.

In order to compare the maximum water content, both the modified and unmodified zeolite samples were equilibrated with free air. After one month of equilibration under identical conditions, the samples were analyzed thermogravimetrically, and mass losses of 23.6 and 20% was noted for the original and modified sample, respectively. The expected drop in water content of the modified sample is not obviously due to a partial occupancy of zeolite cavities by platinum clusters, it is also due to the increase in the content of dry matter after platinum incorporation.

For any electrode material, its electronic conductivity is of essential importance. For that reason, the conductivity of the synthesized samples was checked. In Figure 2 one can see the complex impedance plots of both original and modified dry zeolite 13X recorded at a constant pressure of 1400 kg cm<sup>-2</sup>. The diagrams are somewhat distorted semicircles, characteristic of low conducting materials and extremely low interfacial capacitance. Such diagrams agree with those reported elsewhere for dry zeolites at near-room temperature [11, 29]. The radii of the semicircles are slightly pressure dependent, and those measured at 700 kg cm<sup>-2</sup> are approx. 5% higher,

but also show a more expressed scatter of experimental points. The low frequency cross section of the semicircles where the real impedance axis corresponds to a conductivity of  $0.8 \times 10^{-8} \text{ ohm}^{-1} \text{ cm}^{-1}$  and  $2.5 \times 10^{-8} \text{ ohm}^{-1} \text{ cm}^{-1}$  for the original and modified sample, respectively. This is in the range of the room temperature conductivity of dry zeolites, which is otherwise ionic in nature and originates from sodium ion mobility [29, 30]. The low contribution of metallic platinum to the overall sample conductivity indicates that platinum clusters are short circuited to a very low degree, if at all. This is in accordance with numerous investigations using sophisticated techniques [2 – 11], which showed that one must account for the small clusters placed inside the zeolite cavities. Therefore, it was considered useful to add several percent carbon black to these materials, to enhance the electronic conductivity and to improve its utilization when used as an electrode material.

Since, in this work, zeolite was used in an aqueous medium, the impedance of wet, air-equilibrated samples was also measured. As shown in Figure 3, the complex impedance plot of a wet sample, in a similar frequency range, shows a different behaviour in comparison to that of the dry sample. In this case the impedance diagram is characteristic of surface reactions controlled by diffusion; most probably the O/OH<sup>-</sup> redox pair, due to the presence of OH<sup>-</sup> from dissociated water molecules, and oxygen from air. This type of diagram indicates that the charge transfer impedance, which otherwise produces a semicircle in the region of high frequencies, is strongly overlapped with the diffusion impedance characteristic of the low-frequency region. The conductivity in this case may be calculated as the reciprocal value of the high frequency intercept of the impedance diagram with the real axis, likely in the case of dry zeolite at high temperature [29]. The conductivity estimated in this way for both the original and modified sample is of the order of  $10^{-4} \text{ ohm}^{-1} \text{ cm}^{-1}$ , which evidences the very enhanced mobility of sodium cations in the zeolite cavities of a wet sample. Enhanced ionic conductivity

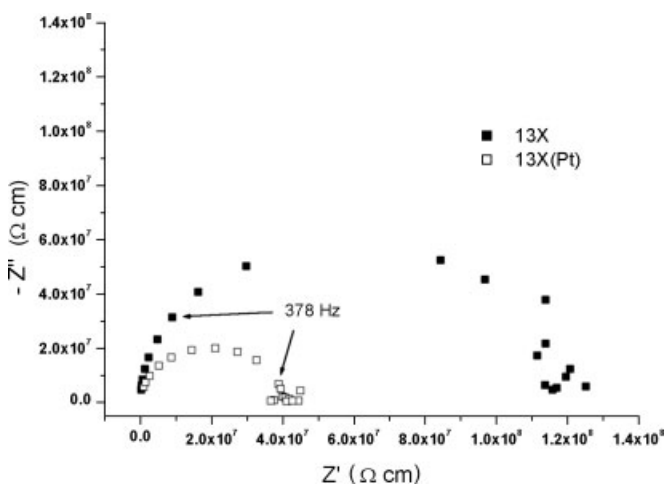


Fig. 2 Complex impedance plot for dry 13X zeolite and platinum modified 13X zeolite pellets, measured at 20 °C, at a constant pressure of 1400 kg cm<sup>-2</sup> in the frequency range 1 – 9500 Hz for 13X, and 6 – 60000 Hz for 13X(Pt).

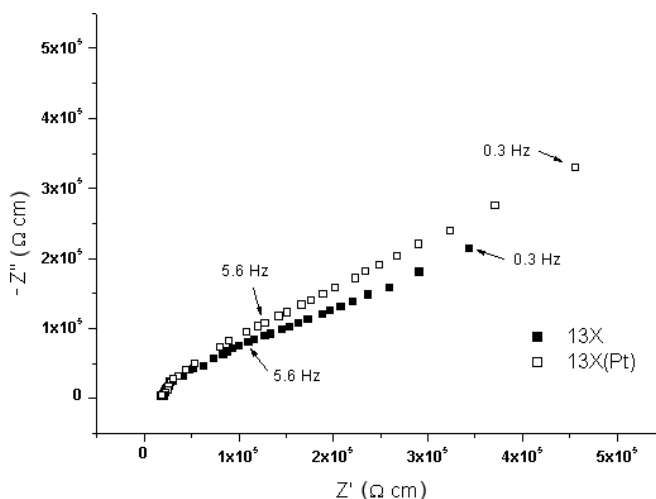


Fig. 3 Complex impedance plot for original 13X zeolite and platinum modified 13X zeolite pellets, measured at 20 °C, at a constant pressure of 1400 kg cm<sup>-2</sup> in the frequency range 0.3–40000 Hz. The samples were saturated with adsorbed water during equilibration in free air for one month.

of wet samples screens the contribution of metallic platinum to the overall conductivity, and therefore for wet samples there is not a substantial difference in the conductivity between the original and the platinum modified sample.

### 3.2 Kinetics of Hydrogen Evolution

Figure 4 shows the voltammograms obtained with Pt/NaX applied to a glassy carbon rotating disc electrode, in dilute sulfuric acid, in the voltage region characteristic of the hydrogen evolution reaction. For the sample with a smaller percentage of carbon black added, or with none at all, in the early phase of voltammetry hydrogen evolution is usually very sluggish, i.e., the currents are very low, but by multiple repeating polarization cycles, the kinetics becomes faster and faster. 10–100 cycles at a polarization rate of  $20 \text{ mV s}^{-1}$  are required to reach maximum current values. This peculiarity of zeolite modified electrodes was also reported by Iwakura et al. [21], who potentiodynamically investigated the  $\text{Fe}^{2+}/\text{Fe}^{3+}$  redox couple inside NaX zeolite cavities in 0.1 M HCl + 0.1 M NaCl water solution. For the sample with 10% carbon black added, the time period required to obtain maximum current is much shorter and corresponds to about 5 polarization cycles.

The electrode material used, due to its developed surface, shows a high interfacial capacitance and consequently very low polarization rates are required to reduce the splitting between the voltammograms recorded in different polarization directions. The rates equal to, or less than,  $1 \text{ mV s}^{-1}$  satisfy this condition. Therefore the voltammograms presented in Figure 4 may be considered as stationary current-voltage curves for hydrogen evolution.

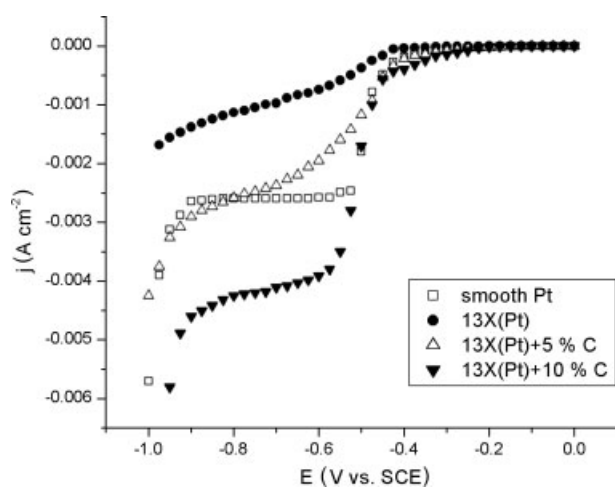


Fig. 4 Stationary current/voltage curves recorded with a rotating disc electrode at  $25^\circ\text{C}$ , using a rotation rate of 10 cps and a polarization rate  $1 \text{ mV s}^{-1}$ . The glassy carbon rotating disc was covered by a thin layer of platinum modified 13X zeolite, to which different percentages (assigned in the inserted legend) of carbon black were added. For the sake of comparison, the voltammogram recorded using a smooth platinum rotating disc is also presented.

For the sake of comparison, the corresponding voltammogram obtained on a smooth platinum rotating disc was also plotted in this figure.

On smooth platinum, hydrogen evolution, involving the protons from  $\text{H}_2\text{SO}_4$ , starts at about  $-0.4 \text{ V}$  vs. SCE, and reaches a diffusion limit at about  $-0.6 \text{ V}$ . Therefore, the Tafel region is between the last two figures. At very negative potentials, extending to  $-0.9 \text{ V}$ , an additional current jump appears, which is due to water splitting.

As one can see in Figure 4, all the Pt/NaX samples also allow hydrogen evolution to start at approx.  $-0.4 \text{ V}$  vs. SCE. However, in respect of the value of the limiting current density, there are substantial differences between the samples containing different amounts of carbon black. The sample without carbon black added, shows a limiting current density substantially (about three times) lower than smooth platinum. The sample with 5% carbon black added, shows very similar hydrogen evolution kinetics to that observed on a smooth platinum electrode. The sample with 10% carbon black added, with a limiting current density in the region ( $-0.6$  to  $-0.9 \text{ V}$ ), enables remarkably (approx. twice) fast hydrogen evolution compared to smooth platinum. That indicates a simple fact, that the utilization of platinum to support hydrogen evolution, as well as the fraction of active electrode surface, depend to a considerable extent on the effectiveness of electronic short-circuiting between the zeolite particles and the glassy carbon support.

To estimate the nature of limiting currents in Figure 4, the voltammograms were recorded at various rotation rates. Figure 5 displays the results of these measurements, for the currents measured at  $-0.75 \text{ V}$ . For a completely reversible, diffusion controlled electrode reaction; the theory of rotating electrodes predicts a rectilinear dependence of limiting current on the square root of angular frequency, which crosses the origin of the coordination system. The nature of the diagrams in Figure 5, for the samples that contain carbon black,

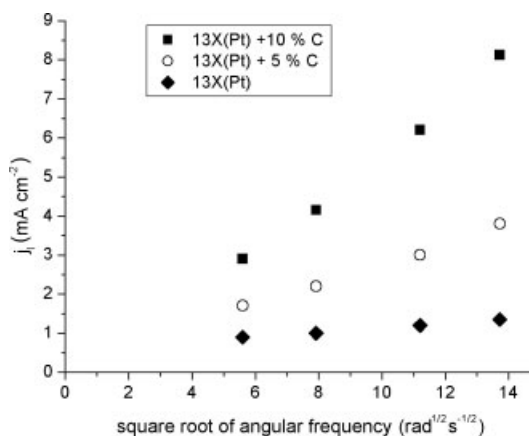


Fig. 5 Dependence of limiting cathodic current density (at  $-0.75 \text{ V}$  vs. SCE) on square root of angular frequency, for a glassy carbon disc covered by a thin layer of platinum modified 13X zeolite, with or without the addition of carbon black, in the mass percentages assigned in the inserted legend.

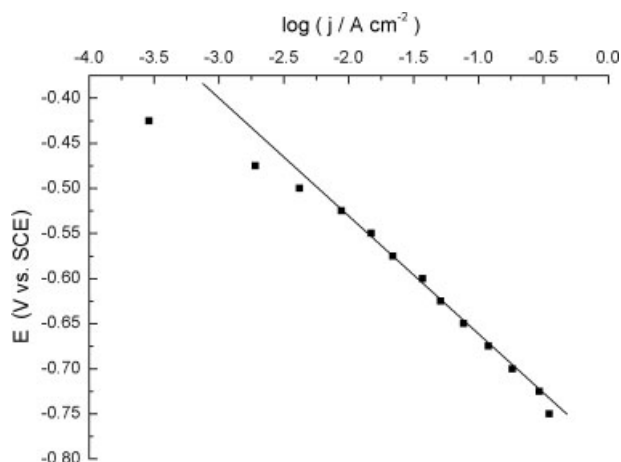


Fig. 6 Potential versus logarithm of cathodic current density plot for stationary current-voltage curve recorded using rotating GC disc covered by thin layer of platinum modified 13 X zeolite with 10% of carbon black added; rotation rate 20 cps.

indicates diffusion control of hydrogen evolution. However, for the sample without carbon black, the limiting current is only slightly dependent on rotation rate, and the diagram does not cross the origin of the coordination system. Therefore, most probably, the limitations in this case originate from the diffusion of hydrogen within the zeolite cavities.

The voltammograms of the zeolite samples, in the region of limiting current, show an enhanced slope toward the voltage axis, in comparison with that obtained on smooth platinum. It is likely that the potential is non-uniformly distributed along the zeolite particles, and therefore all samples show the increase of the surface fraction available to hydrogen evolution with the increase in cathodic polarization.

For the sample with 10% carbon black added, the potential region  $-0.4$  to  $-0.6$  V is obviously a region of mixed, activation diffusion control. This part of the current-voltage diagram was presented in Tafel form (potential versus logarithm of current density) in Figure 6. To enlarge the potential region available for Tafel analysis, the over-voltage was plotted as a function of  $\log [j / (1 - j/j_l)]$  where  $j_l$  is the apparent limiting current density. Unexpectedly for a heterogeneous, dispersed material, the plot is a reasonably straight line with a slope of 135 mV per decade. The formal potential of the hydrogen electrode for 2.5 mM sulfuric acid practically overlaps with the starting point of the voltage axis, and therefore extrapolation of the Tafel line to the  $\log(\text{current density})$  axis gives the logarithm of the apparent exchange current density in this system. From this extrapolation, the value of the apparent exchange current density amounts to  $0.71 \text{ mA cm}^{-2}$ .

## 4 Concluding remarks

This work shows that under the appropriate conditions, platinum modified zeolite may be used to carry the electrochemical reactions relevant to fuel cells, competitively to platinum dispersed on an electronically conductive support, like

to a carbon black. Recently, much attention has been paid to searching for synergistic effects of metal/metal or metal/oxide combinations, in order to minimize the consumption of platinum [26, 31]. Due to their thermal stability in both oxidising and reducing media, zeolite materials offer a number of possibilities for synthesizing different metal/metal or metal/oxide composite materials in the form of a nano-dispersion, in a way similar to that used in this work. The pronounced hygroscopic nature of zeolites presents their notable advantage if used in water based electrolyte solutions.

## Acknowledgement

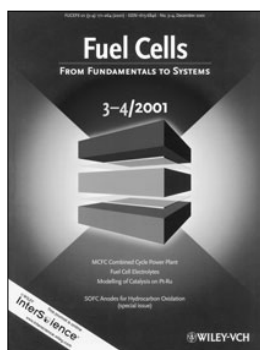
The work was supported by the Ministry of Science, Technology, and Development of the Republic of Serbia, contract No. 1399 (M.S), and contract No. 1713 (Z.T).

M.S. thanks the European Community for financial support (contract No. ICA2-CT-2002-10001). The authors also thank Prof. M. Mitrovic from the Physical Faculty, Belgrade Univ., for the SEM micrographs used in this work.

## References

- [1] D. W. Breck, *Zeolite Molecular Sieves: Structure, Chemistry and Use*, Wiley, New York, 1974.
- [2] A. M. Ferrari, K. M. Neyman, T. Belling, M. Mayer, N. Rösch, *J. Phys. Chem. B* **1999**, *103*, 216–226.
- [3] A. L. Yakovlev, K. M. Neyman, G. M. Zhidomirov, N. Rösch, *J. Phys. Chem.* **1996**, *100*, 3482–3487.
- [4] R. E. Jentoft, M. Tsapatsis, M. E. Davis, B. C. Gates, *J. Catal.* **1998**, *179*, 565.
- [5] Labouriau, G. Panjabi, B. Enderle, T. Pietrass, B. C. Gates, W. L. Earl, *J. Am. Chem. Soc.* **1999**, *121*, 7674.
- [6] W. A. Weber, B. C. Gates, *J. Catal.* **1998**, *180*, 207.
- [7] W. A. Weber, B. L. Phillips, B. C. Gates, *Chemistry a European Journal* **1999**, *5*, 2899.
- [8] W. A. Weber, A. Zhao, B. C. Gates, *J. Catal.* **1999**, *182*, 13.
- [9] P. Gallezot, I. Mutin, G. Dalmai-Imelik, B. Imelik, *J. Microsc. Spectrosc. Electron.* **1976**, *1*, 1.
- [10] P. Gallezot, *Surf. Sci.* **1981**, *106*, 459.
- [11] A. Tonscheidt, P. L. Ryder, N. I. Jaeger, G. Schulz-Eklhoff, *Surf. Sci.* **1993**, *281*, 51.
- [12] A. Tonscheidt, P. L. Ryder, N. I. Jaeger, G. Schulz-Eklhoff, *Zeolites* **1996**, *16*, 271.
- [13] V. Alfredsson, O. Terasaki, Z. Blum, Jan-Olov Bovin, G. Karlsson, *Zeolites* **1995**, *15*, 111.
- [14] M. Hartman, C. Bischof, Z. Luan, L. Kevan, *Micropor.-Mesopor.Mater.* **2001** *44–45*, 385.
- [15] M. Vaarkamp, F. S. Modica, J. T. Miller, D. C. Koningsberger, *J.Catal.* **1993**, *144*, 611.
- [16] S. E. Deutsch, J. T. Miller, K. Tomishige, Y. Iwasawa, W. A. Weber, B. C. Gates, *J.Phys.Chem.* **1996**, *100*, 13408.
- [17] D. Barthoment, *Catal.Rev.* **1996**, *38*, 521.

- [18] U. Simon, M. E. Franke, *Micropor. Mesopor. Mater.* **2001**, 41, 1.
- [19] M. Xu, W. Horsthemke, M. Schell, *Electrochim.Acta* **1993**, 38, 919.
- [20] Z. Li, C. M. Wang, L. Persaud, T. E. Mallouk, *J.Phys.Chem.* **1988**, 92, 2592.
- [21] C. Iwakura, S. Miyazaki, H. Yoneyama, *J.Electroanal.-Chem.* **1988**, 246, 63.
- [22] D. R. Rolison, E. A. Hayes, W. E. Rudzinski, *J.Phys.Chem.* **1989**, 93, 5524.
- [23] L. Keck, J. S. Buchanan, G. A. Hards, *U.S.Patent* 5,068,161, **1991**.
- [24] M. S. Wilson, Membrane catalyst layer for fuel cells, *U.S.Patent* 5,234,777, **1993**.
- [25] T. R. Ralph, G. A. Hards, J. E. Keating, S. A. Campbell, D. P. Wilkinson, M. Davis, J. St-Pierre, M. C. Johnson, *J.Electrochem.Soc.* **1997**, 144, 3845.
- [26] T. R. Ralph, M. P. Hogarth, *Platinum metals review* **2002**, 46, 3.
- [27] S. R. S. Prabaharan, S. S. Michael, C. Julien, *Int.J.Inorg.-Mat.* **1999**, 1, 21.
- [28] Young-Min Choi, Su-Il Pyun, Joon-Sung Bae, Seong-In Moon, *J.Power Sources*, **1995**, 56, 25.
- [29] N. Cvjeticanin, S. Mentus, N. Petranovic, *Solid State Ionics* **1991**, 47, 111.
- [30] D. N. Stamires, *J.Chem.Phys.* **1962**, 36, 3174.
- [31] M. M. Jaksic, *Solid State Ionics* **2000**, 136-137, 733-746.



## Tables of Contents by E-Mail

Find out what's in the latest issue through automatic notification. Wiley InterScience now offers free content alerts to all Registered Users – no subscription required. To activate your e-mail alerts for this journal, login to Wiley InterScience, go to the journal, and click on the ADD ALERT button on the “Available Issues” page.